ISSN 1392-1207. MECHANIKA. Vol. 29, No. 2, 2023: 97–103

Numerical Estimation of the Influence of Pre-Induced Micro-Cracks in the Stress Concentration Zone on the SIFs of a Lower Suspension Arm

Kishorekanna GUNASEKARAN*, Isaac SOLOMON, Gintautas DUNDULIS*****
**Kaunas University of Technology, Faculty of Mechanical Engineering and Design, Studentų st. 56, LT-51424 Kaunas, Lithuania, E-mail: kishore.gunasekaran@ktu.edu*
***Kaunas University of Technology, Faculty of Mechanical Engineering and Design, Studentų st. 56, LT-51424 Kaunas, Lithuania, E-mail: isaac.micheal@ktu.edu*
****Kaunas University of Technology, Faculty of Mechanical Engineering and Design, Studentų st. 56, LT-51424 Kaunas, Lithuania, E-mail: gintautas.dundulis@ktu.lt*
https://doi.org/10.5755/j02.mech.31660

1. Introduction

Suspension lower arm is an automotive component that is used to maintain the stability of the wheel whenever it goes up a road bump, goes down on potholes, cornered, braked, and drifted. Typically the suspension arm attains two types of loadings, Road disturbance and Load disturbance [1]. Either of them has certain circumstances at which they exceed loading limits and cause discrepancies in the component. The importance of studying the fatigue characteristics of this component tends to be very crucial as fatigue cracks and failure are often observed in the component due to excessive loads.

Previously after conducting fatigue, dynamic and kinematic analysis, Optimisation has been done on the suspension system, but its failure is some part that has still been unstudied [2]. Though the research conducted is based on the load that displaces the arm when the vehicle is at rest, random vibration analysis can be performed, and the obtained response equations can be applied as a load spectrum with different amplitude loading to partially resemble real-time loading conditions [3]. Through these simulations, the vibrational fatigue experienced by the component can be evaluated [4].

In engineering practice, the highest stress region of construction element is determined and compere with fatigue strength due to avoid fatigue crack [5] as it is the most vulnerable region during cyclic loads. Fatigue cracks may also arise due to misconstructions, wrong fatigue strength calculations and manufacturing flaws [6] which in the end account for the failure of the component. Stress Intensity Factor (SIF) plays a key role in fracture mechanics as it a factor related to the crack growth rate [7]. Determining the stress state (SIF) near the tip of the crack is significant to determine the zone (tension or compression) under which the crack propagates. Negative SIF results the crack under compressive concentration zone [8] which has minimal impact on crack growth rate that too when the tensile forces due to internal stress exceed remote compressive stress near the crack.

This research study of integrating the concept of fracture mechanics and the evaluation of Stress Intensity Factors (SIF) in the stressed zones of the lower suspension arm is a novel approach and helps in estimating the structural response of components induced with micro-cracks in the stress concentration zone. This numerical study provides sufficient data on the mechanical behaviour of the lower suspension arm simulating loading conditions under a constant amplitude depending on the load that displaces the component when the vehicle is at rest and the effect of the stress intensity factors at the pre-induced crack regions [9, 10]. The results obtained in the research help to configure the most vulnerable crack and is at risk of failure at their respective assigned mode.

2. Methodology

The below Fig. 1 displays a real-time model of a front axle lower suspension arm. It is made of AISI 1018 steel with two of its ends constrained and the other end is connected to the ball joint of wheel.

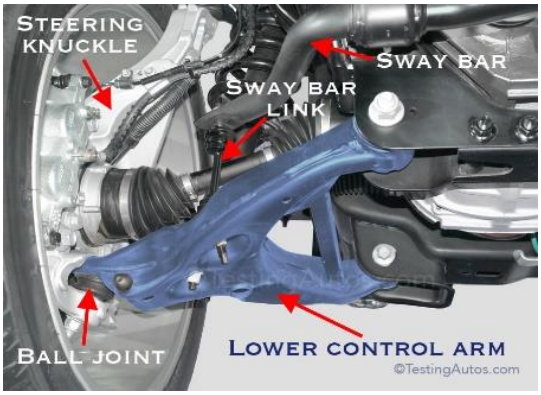

Fig. 1 A-type suspension lower arm [11]

The force that acts on the component is split into 4 individual modes to resemble real loading conditions [11]. The A-type suspension lower arm of a Kia Sorento is considered, and it has been optimised and given additional design support at the ribs under the horizontal bar [12]. The initial design of the arm is modelled in Solidworks 2020 Software. Analytical calculations are performed to estimate the force that acts on the suspension lower arm at the front axle. It is found that there are 4 modes that act on the component: Vertical bumping, braking, cornering, and lateral loading. These 4 modes of loading have independent boundary conditions as they tend to act at different mechanisms of the component. The computational model is then transferred to Ansys 2021 R1 software for performing the finite element numerical simulations.

Initially, the basic boundary conditions are set according to the load that displaces the component when the vehicle is at rest and the static simulation is carried out [13].

It is found that the model possesses five different zones where stress is subjected to maximum conditions. When the suspension arm is subjected to unstable loads, it has the possibility to fracture at any of these points.

Hence this research aims at providing strength-based estimates by inducing micro surface cracks on the five critical stress concentrated regions and evaluate their stress intensity factors. The crack consists of six Contours, all the same dimensions having 0.1 mm major and minor radii, The largest contour radius 0.005 mm. The research gives conclusive evidence of the structural response of the numerically simulated crack-induced component and the estimated crack growth rate at the crack-induced regions based on the SIFs at the stress concentration zones.

3. Analytical approach

The Analytical calculations are performed to determine the forces acting on the wheels. The Suspension Lower Arm is made up of AISI 1018 Steel.

3.1. Static axle load

The front suspension attachment structure retains the suspension at several points like the shock absorber, spring, and control arm [14]. The modes which provide dominant structural requirements include braking, cornering, roll over and vertical bump.

1. Modes of use; Braking, Cornering, roll over and vertical bump.

2. Loads being applied; In this computational study, we initially consider the maximum loads at the tire path during these modes, and then using static equilibrium of the suspension and determine the maximum loads at the body attachment points.

For the vehicle at rest: Using static equilibrium, the front and rear tire patch loads, R_f and R_r, may be determined as:

$$R_f = \frac{b}{a+b}\frac{W}{2} \text{ and } R_r = \frac{a}{a+b}\frac{W}{2}, \quad (1)$$

where: R_f is the vertical load at a front tire patch; R_r is the vertical load at a rear tire patch; W is the vertical weight

While a and b are the dimension of the vehicle from the centre of the car to the from and back axles. For the dimensions of Kia Sorento a – 1397.5 mm, b – 1297.5 mm and weight – 2590 kg. Applying the estimation in Eq. (2) the obtained results stand as $R_f = 1247$ N; $R_r = 1862$ N.

The value of R_f can be considered as load experienced by the front axle of the lower control arm during bumping mode (at rest or at a constant velocity) or the default load that tends to displace the component to some extent.

3.2. Braking mode

Considering a steady-state braking deceleration of 10 times the acceleration due to gravity, using static equilibrium, the front axle load at the tire patch can be estimated from:

$$F_f = \left(\frac{b+nh}{a+b}\right)\mu\frac{W}{2}, \quad (2)$$

where: F_f is front – aft load at front tire patch; n is braking deceleration in g's; μ is coefficient of friction between tire and road = 0.7 (considering dry road); h is height of CG above ground = 850 mm. Thus $F_f = 3295$ N.

For the maximum fore-aft tire patch loading during braking mode, the loads at the lower control arm ball joint are estimated from:

$$A_{fa} = \left(\frac{r-c}{d}+1\right)F_f, \quad (3)$$

where: A_{fa} is Fore – aft lower control arm load at ball joint; F_f is Fore – aft load at the tire patch; r, c, d are dimensions shown in Fig. 2.

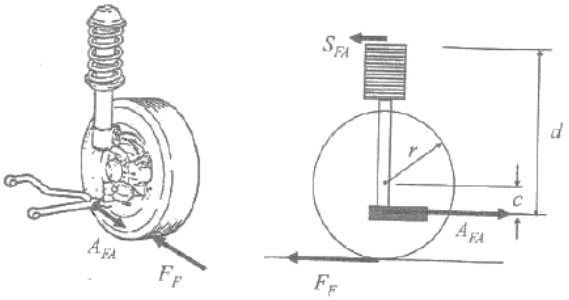

Fig. 2 Suspension fore - aft loading at ball joint [15]

From Fig. 2., the dimensions r, c and d for Kia Sorento; r is 2413 mm; c is 1050 mm; d is 4871 mm.

When the vehicle is decelerated by 1g, the load that acts on the lower suspension arm ball joint is 4217.8 N. This can vary depending on the deceleration of the vehicle.

3.3. Cornering and roll-over

When rollover of the vehicle is incipient during cornering, the steady state resultant acceleration at the centre of gravity begins to go outside the base of the vehicle track [16], then the lateral tire patch at the front axle is:

$$L_0 = \left(\frac{2h}{t}\right)W_f. \quad (4)$$

The calculated value of $L_0 = 2675$ N, for the maximum lateral tire patch load during rollover mode:

$$A_l = \left(\frac{r-c}{d}+1\right)L_0, \quad (5)$$

where: A_l is the lateral lower control arm at the body attachment, r, c, d are the dimensions shown in Fig 3. L_o is the lateral load of tire pitch.

When the vehicle is corned at 1g, the lower suspension arm experiences a lateral load of 3423 N at the ball joints. For the vertical bumping mode, the normal force attained can be obtained as R_f = 1247 N from Eq. (2). Three maximum loads during braking, cornering rollover and lateral loading is considered individually for analysis in their

respective directions as they tend to cause fatigue in the component.

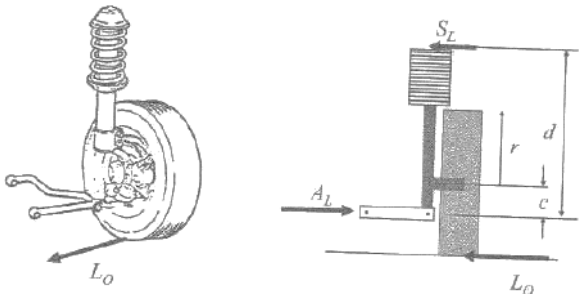

Fig. 3 Suspension lateral loading [15]

The micro-cracks that are intentionally induced in the model are based on the stress analysis and simulation of bumping mode as this reveals the force acting on Lower control arm when the vehicle is at rest or moving in a constant velocity. The other modes are also common, but their values obtained are 10 time the acceleration due to gravity, so they are used to obtain the behaviour of the component under maximum loads at each mode. This estimated the SIF of the micro-cracks from which it was initially formed depending on the bumping mode stress concentration zones.

4. Computational modelling

The three-dimensional Linear elastic finite element model was generated in ANSYS workbench using a structured meshing technique for creating quadratic hexahedral elements.

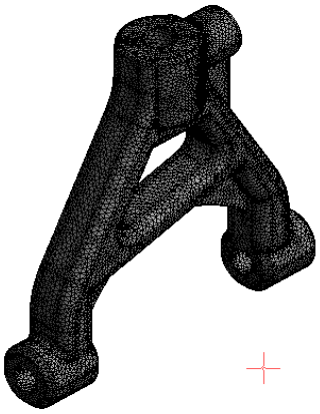

Fig. 4 Meshed Isometric view of component

4.1. Static simulation

This presents the static simulation of the Suspenion Lower Arm where the two joint are constrained in the bushings and the other joint is connected to the ball joint where the force acts [17]. The value of force 1247 N derived from the analytical calculations are used as the input load (force) for the numerical study and the simulation is carried out under quasi static loading.

The below Fig. 5 presents the equivalent stress of the component in standard conditions. The maximum stress is found to be 20.726 MPa.

It is well below the yield stress and extremely safe for normal static conditions. In these normal static conditions, five individual stress concertation zones are estimated. The maximum points tend to be near the edges of the Suspension Lower arm, this shows that there is a possibility of fracture at any of these five points whenever the component is subjected to excessive loads. The fracture may occur depending on the pothole or road bumps and how the driver handles these conditions. Individual micro-cracks of the same dimensions are to be induced and analysed.

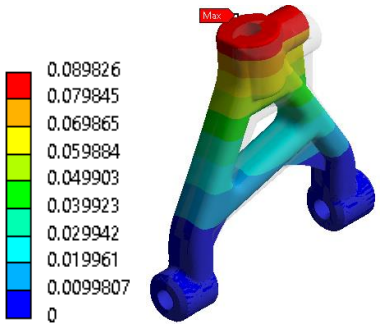

a

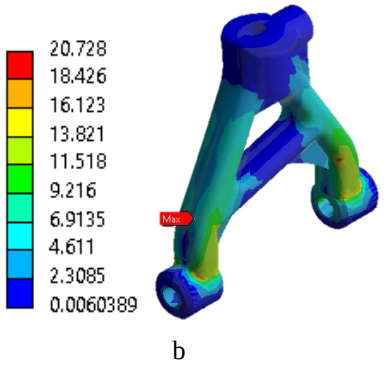

b

Fig. 5 Results of static simulation: a) total deformation; b) stress distribution

4.2. Estimation of stress concentration zones

The below Fig. 6 presents 5 co-ordinate systems which marks the locations of the micro-fractures in the component. All the cracks were induced perpendicular to the Maximum Principal stress concentration zones which marks the most vulnerable regions and prone for fatigue cracks [18]. Semi-elliptical micro cracks totally consisting of 6 contours with 0.1mm major and minor radii are to be induced. Mesh element type for generating surface cracks on the component is Hex-Dominant.

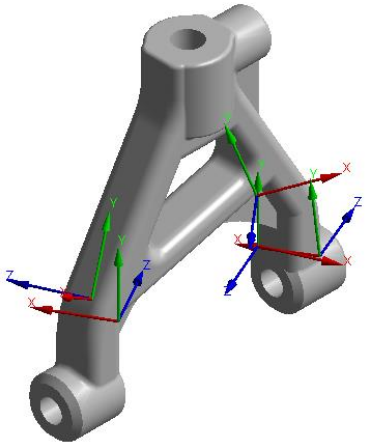

Fig. 6 Location of Micro-fractures

The below Fig 7. presents the isometric zoomed view of the semi-elliptical crack induced in the component.

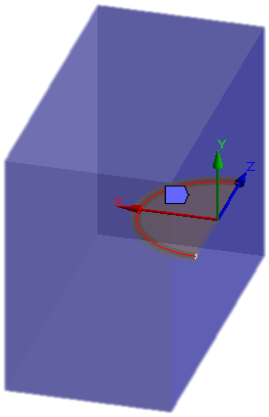

Fig. 7 Isometric view of induced semi-elliptical crack

Each surface crack is simulated individually to characterise the behaviour of the respective crack in each mode and the obtained results are tabulated for final comparison.

5. Results

The stress intensity factor, is used in fracture mechanics to predict the stress state near the tip of a crack or notch caused by a remote load or residual stresses. [19].

The numerically solved SIF results are analysed separately in 4 different modes, the crack with maximum SIF has the highest possibility to propagate and fail first. Another important note is that if the SIF is negative for a crack, it is under a compressive stress concentration zone which makes the notch of crack compress instead of propagating [20].

In this research, only the propagation of the crack notch with respect to SIF is studied and analysed in each mode. The surface cracks under a compressive concentration zone may have different impact on the components behaviour but is neglected for this research.

5.1. Bumping mode

From the above Table 1, it is seen that cracks 1, 2 and 3 are under a compressive stress concentration zone when the vehicle induced with micro-cracks is at rest or in a constant velocity. Even if bumping occurs the compressive state does not change, the only thing that changes is the SIF of the cracks. This also applies for the cracks 4 and 5, depending on the bump and force the SIF may change but they are no longer going to have negative SIF. Comparing the positive values of cracks 4 and 5, Crack 4 has the highest SIF and has the possibility to propagate more than crack 5 in normal bumping conditions.

Table 1

Resultant values of the numerical study for different cracks in Bumping mode

Crack no.	Resultant values	
	Maximum SIF, MPa.mm^(0.5)	Minimum SIF, MPa.mm^(0.5)
1	-5.421	-6.394
2	-7.976	-9.427
3	-8.045	-9.364
4	8.177	7.013
5	5.264	4.812

Observing the Von-mises stress of the component with the induced crack, the maximum stress always by far exceeds the ultimate tensile strength of the component and tends to act at the notch of the crack which remarks feasible propagation [21]. The crack 4 has the highest propagation rate in this mode and does not apply to all the modes as they all subject to have different boundary conditions, and the direction of the forces that act on them vary depending on the mode.

5.2. Braking mode

The Fig. 8 displays the von-Mises stress distribution of the suspension lower arm in braking mode without induced cracks when a force equivalent to 10 times accelaration due to gravity is applied to decelerate the vehicle.

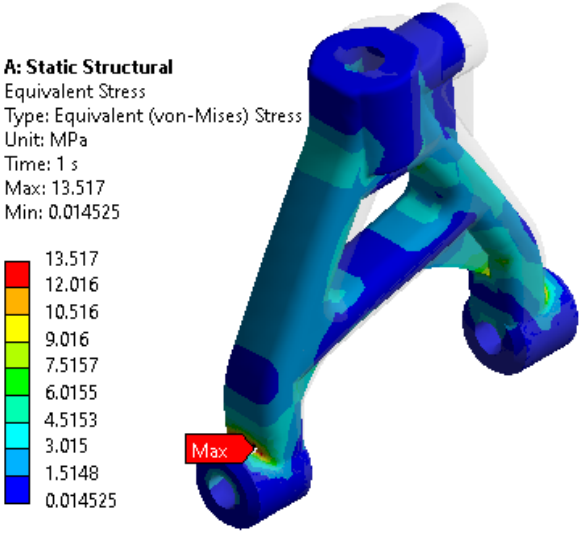

Fig. 8 Von-Mises stress distribution in Braking mode without induced micro-cracks

Table 2

Resultant values of the numerical study for different cracks in Braking mode

Crack no.	Resultant values	
	Maximum SIF, MPa.mm^(0.5)	Minimum SIF, MPa.mm^(0.5)
1	-0.375	-0.439
2	3.206	2.728
3	-3.697	-4.288
4	2.744	2.346
5	-1.086	-1.227

In Braking mode, it is observed that the Cracks 1, 3 and 5 have negative SIF which concludes they are under a compressive stress concentration zone which makes the no way for the crack to propagate. Cracks 2 and have a positive SIF in which Crack 2 has a larger SIF when compared to Crack 4. Hence, it is concluded that Crack 2 has the highest SIF in Braking mode and has the highest propagation rate.

5.3. Incipient cornering mode

In Cornering mode, observation reveal that Cracks 2 and 4 have negative SIF which says they are under a compressive stress concentration zone which makes the no way for the crack to propagate [16].

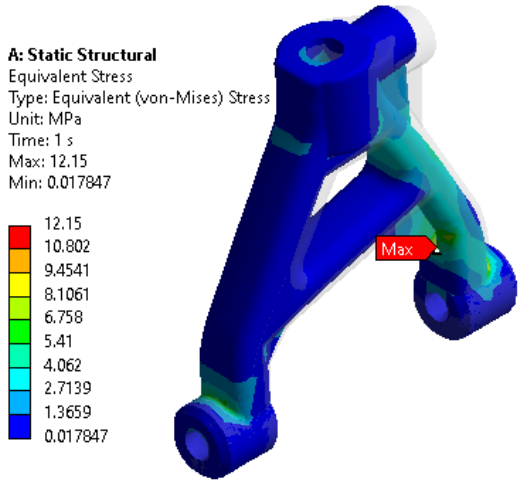

Fig. 9 Von-Mises stress distribution in Cornering mode without induced micro-cracks

Table 3

Resultant values of the numerical study for differnt carcks in Cornering mode

Crack no.	Resultant values	
	Maximum SIF, MPa.mm^(0.5)	Minimum SIF, MPa.mm^(0.5)
1	0.062	0.039
2	-2.986	-3.511
3	1.433	2.136
4	-2.062	-2.411
5	0.391	0.338

Cracks 1, 3 and 5 have a positive SIF in which Crack 3 has a larger SIF when compared to Cracks 1 and 5. So it is concluded that Crack 3 has the highest SIF in cornering mode and has the highest propagation rate.

5.4. Lateral load mode (roll-over)

In Lateral load mode, it is seen that no cracks are under compressive concentration zone, all the cracks have a positive crack growth rate. Out of which Crack 2 has more SIF when compared to the all the other cracks. Hence, it is concluded that Crack 2 has the highest SIF in Lateral load mode and possess the highest propagation rate.

Numerical comparison of SIF is shown in Fig. 11.

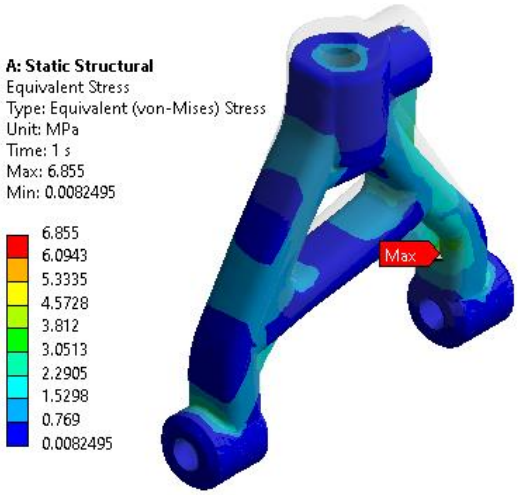

Fig. 10 Von-Mises stress distribution in roll-over mode without induced micro cracks

Table 4

Resultant values of the numerical study for differnt carcks in Lateral mode

Crack no.	Resultant values	
	Maximum SIF, MPa.mm^(0.5)	Minimum SIF, MPa.mm^(0.5)
1	0.298	0.253
2	1.891	1.607
3	1.646	1.418
4	0.858	0.734
5	0.494	0.447

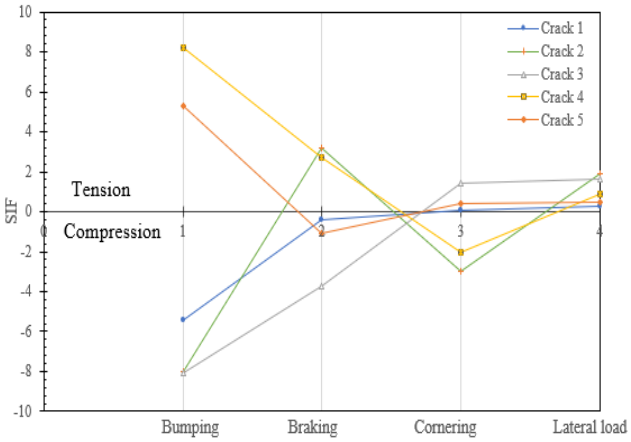

Fig. 11 Comparison of SIF in all modes

6. Conclusion

Lower suspension arm is an important component of the suspension system of the vehicle [12], this research studies the structural response of a lower suspension arm induced with multiple micro-cracks in the stress concentration zones during normal bumping mode. From the analytical calculations, it is seen that the lower control arm can be subjected to fatigue failure in 4 different modes and the maximum forces attained in these modes are obtained with an estimation of 10 times the acceleration due to gravity. The values are approximate as the exact force applied on the component depends on the condition of the road and driving environment.

The maximum value of SIF in each mode may be considered as a ratio for the crack propagation and when the acceleration due to gravity is doubled or halved, the values of the SIF may change with similar ratio depending on the exerted force. From the SIF of crack 2 in braking mode, independent of the times of force applied, crack 2 estimates the highest crack growth rate. Compressive concentration zone plays an important role in this research as the SIF in negative estimates of the crack eliminates it from the crack growth rate. The estimates of SIF if negative, will have a substantial impact on the von-mises stress at the edge of the notch and equivalent strain but will not alter its crack growth rate.

In conclusion, if there are considerate presence of micro-cracks formed by the excessive amount of stress during the vertical bump mode or normal mode, the crack 4 region will have the highest crack growth rate if the component continues to experience excessive amount of stress during the bumping mode. Crack 2 has the highest crack growth rate if the component continues to experience excessive

amount of stress in the braking mode. Crack 3 has the highest crack growth rate if the component experiences excessive amount of stress in the cornering mode. Crack 2 has the highest crack growth rate if the component experiences excess amount of stress in the lateral loading mode.

Micro- cracks can be formed in any of the maximum Stress concentration zones of the component, but low cycle fatigue depends on the excessive loads it experiences to determine the specific crack which might have the highest crack growth rate. From this research each mode with highest SIF has been evaluated and an estimate is given about the crack growth rate in each mode. SIF is considered in a dependable ratio form and may subject to change abruptly depending on application of forces.

References

1. **M. Sadiq A. Pachapuri; Ravi G. Lingannavar; Nagaraj K. Kelageri; Kritesh K. Phadate.** 2021. Design and analysis of lower control arm of suspension system, Materials Today: Proceedings 47: 2949-2956. http://doi.org/10.1016/j.matpr.2021.05.035.
2. **Saurabh D. Shinde; Shruti Maheshwari; Satish Kumar Ebrahimi.** 2018. Literature review on analysis of various Components of McPherson suspension, Materials 5(9): 19102-19108 https://dx.doi.org/10.1016/j.matpr.2018.06.263.
3. **Shahrum Abdullah; Ahmad Kamal Ariffin; Mohammad Hosseini Fouladi.** 2011. Dynamic Analysis of an Automobile Lower Suspension Arm Using Experiment and Numerical Technique, ResearchGate chapter. https://dx.doi.org/10.5772/13408.
4. **Strzelecki, P.; Wachowski, M.** 2022. Effect of the stress concentration factor on the final fracture zone of aluminium AW 6063 T6 for rotating bending specimens, Materials 31. https://doi.org/10.1016/j.mtcomm.2022.103766.
5. **Richard, H. A; Fulland, M.; Sander, M.; Kullmr, G.** Examples of Fatigue Crack Growth in Real Structures. https://dx.doi.org/10.1016/j.ijfatigue.2012.02.013.
6. **Muhamad, M. N.** 2009. Fatigue life prediction of lower suspension arm using strain-life approach, European Journal of Scientific Research 30(3): 437-450. https://portal.issn.org/resource/ISSN/1450202X.
7. **Vivekanandan, N.; Gunaki, A.; Acharya, C.; Gilbert, S.; Bodak, R.** 2014. Design, analysis and simulation of double wishbone suspension system, IPAS International Journal of Mechanical Engineering 2(6). http://dx.doi.org/10.1088/1757-899X/748/1/012020.
8. **Stepnova, L.; Belova, O.** 2022. Stress Intensity Factors of Continuum Mechanics at the Nanoscale, Procedia Structural Integrity 37: 900-907. https://dx.doi.org/10.1016/j.prostr.2022.02.024.
9. **Muhamad, M. N.; Noor, M. M.; Kadirgama, K.; Bakar, R.; Rejab, M.** 2009. Finite Element Modelling, Analysis and Fatigue Life Prediction of Lower Suspension Arm, Malaysian Technical Universities Conference on Engineering and Technology. https://dx.doi.org/10.4028/www.scientific.net/AMR.264-265.1557.
10. **Rahman, M.;** et al. 2010. Robust design of suspension arm based on stochastic design improvement, 2nd International Conference on Mechanical and Electronics Engineering (ICMEE) 5558508. https://dx.doi.org/10.1109/ICMEE.2010.5558508.
11. **Gadade, B.; Todkar, R.G.** 2015. Design, analysis of A-type front lower suspension arm in Commercial vehicle, International Research Journal of Engineering and Technology 02(07). https://portal.issn.org/resource/ISSN/2395-0072.
12. **Jianpeng Shi; Xin Guan**. 2013.Fatigue life analysis of lower suspension arm, Qiche Gongcheng/Automotive Engineering. https://portal.issn.org/resource/ISSN/1000680X.
13. **Kim, J.; Lei, L.; Kang, B.** 2003. Preform design in hydroforming of automobile lower arm by FEM, Journal of Materials Processing Technology 138(1–3): 58-62. https://dx.doi.org/10.1016/S0924-0136(03)00049-9.
14. **Salih, W. M.** 2011. A novel design of lower vehicle arm based on optimization technique, International Journal of the Physical Sciences 6(4): 768-776. https://doi.org/10.5897/IJPS10.656.
15. **Donal, E. Malen.** 2011. Fundamentals of Automobile Body Structural Design. https://dx.doi.org/10.4271/r-394.
16. **Hamzi, N. M.; Singh, S. S. K.** 2021. Durability assessment of automobile lower arm under random road loads in time-frequency domain, Journal of Failure Analysis and Prevention 21(6): 1973-1980. https://dx.doi.org/10.1007/s11668-021-01255-y.
17. **Mohd Hafizi Abdul Rahman**; **Mohd Shukor Salleh; Mohd Suffian Ab. Razak;** et al. 2018. Design and Optimization of Front Lower Control Arm (FLCA) for C-Segment Passenger Car, International journal of Engineering & Technology 7(3.17). https://dx.doi.org/10.14419/ijet.v7i3.17.16625.
18. **Ritiesh Vasamshetty; Arunkumar, S.** 2022. Stress intensity factor estimation of cracks originating from square, circular or elliptical hole in a plate subjected to tension, Materials 66(4): 1955-1960. https://doi.org/10.1016/j.matpr.2022.05.430
19. **Guebum Han; Kang Min Lee; Seong Keol Kim.** 2014. A study on improving dynamic characteristics of a front lower suspension arm and aerodynamic effects of a handmade hybrid-vehicle, International Journal of Precision Engineering and Manufacturing 15: 1897-1908. https://dx.doi.org/10.1007/s12541-014-0544-1.
20. **Abdelhamid Saoudi; Mohamed Bouazara; Daniel Marceau**. 2011. Fatigue failure study of the lower suspension arm using multiaxle criterion of the strain energy density, Journal of Mechanical Engineering 57(4): 345-356. https://doi.org/10.5545/sv-jme.2009.074.
21. **S. Arun Kumar; Balaji**, **V.** et. al. 2016. Analysis, and optimisation of lower control arm in front suspension system, International Journal of Chemical Sciences 14(2). https://portal.issn.org/resource/ISSN/0972768X.

K. Gunasekeran, I. Solomon, G. Dundulis

NUMERICAL ESTIMATION OF THE INFLUENCE OF PRE-INDUCED MICRO-CRACKS IN THE STRESS CONCENTRATION ZONE ON THE SIFS OF A LOWER SUSPENSION ARM

S u m m a r y

Structural steel is ductile in nature, this is the reason it is used in most of the Sectors in the manufacturing industry. Despite its structural strength, it faces compelling and challenging failures due to unstable, fatigue, dynamic and shock loads.

This research study evaluates the structural response on one of these real-world loading conditions using the finite element method. The design of a lower suspension arm of an automobile is modelled in Solidworks 2020 and is solved for static elastic conditions in Ansys 2021 R1. A set of pre-induced fractures are then integrated into the computational model in the Stress concentration zones in different parts of the body and solved independently. A total of five micro-cracks are induced with each crack consisting of six contours. For the numerical simulation of lower suspension arm, real-time loading conditions must be attained to resemble real-world loading scenario. Hence, 4 modes of solving were chosen which would depict the real-world failure scenario where the suspension lower arm can attain maximum loads. The maximum load values are estimated in each mode and is integrated into the model with predefined boundary conditions for the computational approach.

A detailed numerical comparative conclusion is drawn regarding the SIFs of every mode and the crack that pertains maximum crack propagation rate.

Keywords: lower suspension arm, SIF, crack, analytical, simulation.

Received June 28, 2022
Accepted April 5, 2023